

We are IntechOpen, the world's leading publisher of Open Access books Built by scientists, for scientists

6,900

Open access books available

186,000

International authors and editors

200M

Downloads

Our authors are among the

154

Countries delivered to

TOP 1%

most cited scientists

12.2%

Contributors from top 500 universities



WEB OF SCIENCE™

Selection of our books indexed in the Book Citation Index
in Web of Science™ Core Collection (BKCI)

Interested in publishing with us?
Contact book.department@intechopen.com

Numbers displayed above are based on latest data collected.
For more information visit www.intechopen.com



Land Use Change Monitoring and Modelling using GIS and Remote Sensing Data for Watershed Scale in Thailand

Patchareeya Chaikaew

Additional information is available at the end of the chapter

<http://dx.doi.org/10.5772/intechopen.79167>

Abstract

Landsat 7 Enhanced Thematic Mapper (ETM), Landsat 8 Operational Land Imager (OLI) and Thermal Infrared Sensor (TIRS) images obtained in 1991, 2005 and 2014 with maps, and field survey data were used to classify land use and land cover (LULC) changes over 23 years and predict soil erosion risk locations in the Khlong Kui watershed (73,700 ha), Prachuap Khiri Khan province, Thailand. Classified images together with soil features, slope and rainfall data were used to identify potential risk areas of soil erosion. Based on field check data, the overall classification accuracy was assessed from random samples that resulted as 80% for 1991, 83% for 2005 and 86% for 2014. The study discovered that rice field and rangeland increased by 1.12 and 2.81%, respectively, deciduous forest, and on the other hand, it decreased by 8.28%. GIS analysis identified the potential risk areas of soil erosion as 46,431 ha (0.63%) at very high risk.

Keywords: landsat, DEM, land use land cover, watershed, remote sensing, GIS, soil erosion

1. Introduction

Since the 1990s, global, regional and local studies of land use and land cover changes (LULCC) have greatly developed, thanks to advances in earth observation and monitor methods including remote sensing and GIS techniques. The matter of land use changes has been measured in many international and interdisciplinary researches such as remote sensing, environment and biogeography [1, 2].

In Southeast Asia, including Thailand, deforestation has been occurring during the last 15 years because of an increase in agricultural crops [3]. Land use land cover change in Prachuap Khiri Khan province was reported by the Office of Agriculture Economics (OAE) in 2014 that deforestation has been occurring 6.96% while agriculture and other land use increase 34.97 and 45.44% respectively [4].

Recently, remote sensing is widely applied for monitoring changes and dynamics in land use and land cover (LULC) observation and its impact to the environment. It offers a variety of benefits in LULC study and an opportunity to assess remote area such as tropical forest, high mountains, update land and terrain information and explore historical LULC. To offer more efficiency in identifying land cover changes, remote sensing is often combined with Geographic Information System (GIS) technique. GIS technology refers to for analyzing and managing spatial and temporal data associated with their features [5]. Both technologies provide capability to collect land use characteristics and changes by integrating existing remotely sensed data and relevant environments such as tropical forests, urban areas and coastal zone and different land transformations such as deforestation, urban development and desertification [2, 6–8]. This study shows environmental problems such as deforestation and soil erosion in Thailand caused by human activities. The results of this study could support local governments, local residents and farmers to focus on environmental problems in their regions. The erosion risk map can be used as the potential disaster information to establish field experiments plots for warning the risk area of soil erosion.

2. Data and methods

2.1. Study area

The Khlong Kui watershed is a large watershed in the Southwestern Thailand and is located between $11^{\circ} 58'16''\text{N}$ and $12^{\circ}15'50''\text{N}$ and between $99^{\circ}31'56''\text{E}$ and $99^{\circ}58'30''\text{E}$ as mapped in **Figure 1**. The entire area of the watershed covers approximately 73,700 ha (460,625 rai) in Kui Buri district, Prachuap Khiri Khan province, Thailand. Khlong Kui watershed, with the main river of the watershed, named the Kui Buri River, is surrounded by three main watersheds as (1) Pran Buri; (2) Khlong Khao Daeng and (3) Khlong Saphan Yai of the Prachuap Khiri Khan coast basin, the major river basin in Thailand.

Topography: Khlong Kui watershed includes high mountain range (max. 958 m) on the West, hilly and rolling land, plain and floodplain to the cost on the East as presented in **Figure 1**. High mountain ranges, the major landscape of the Khlong Kui watershed, are mostly in the upper watershed and are mostly covered by forest. Forests in these areas are strictly conserved as water sources. Plains, which cover a small part of the watershed, are used for crop, orchard, and vegetable cultivations. Floodplains, the second large landscape, surround the main rivers and are mostly located in the lower watershed. These areas are generally used for rice cultivations. Deforestation and soil erosion are the major environmental problems in the watershed. These problems are more prominent in the mountain ranges and hilly and rolling lands.

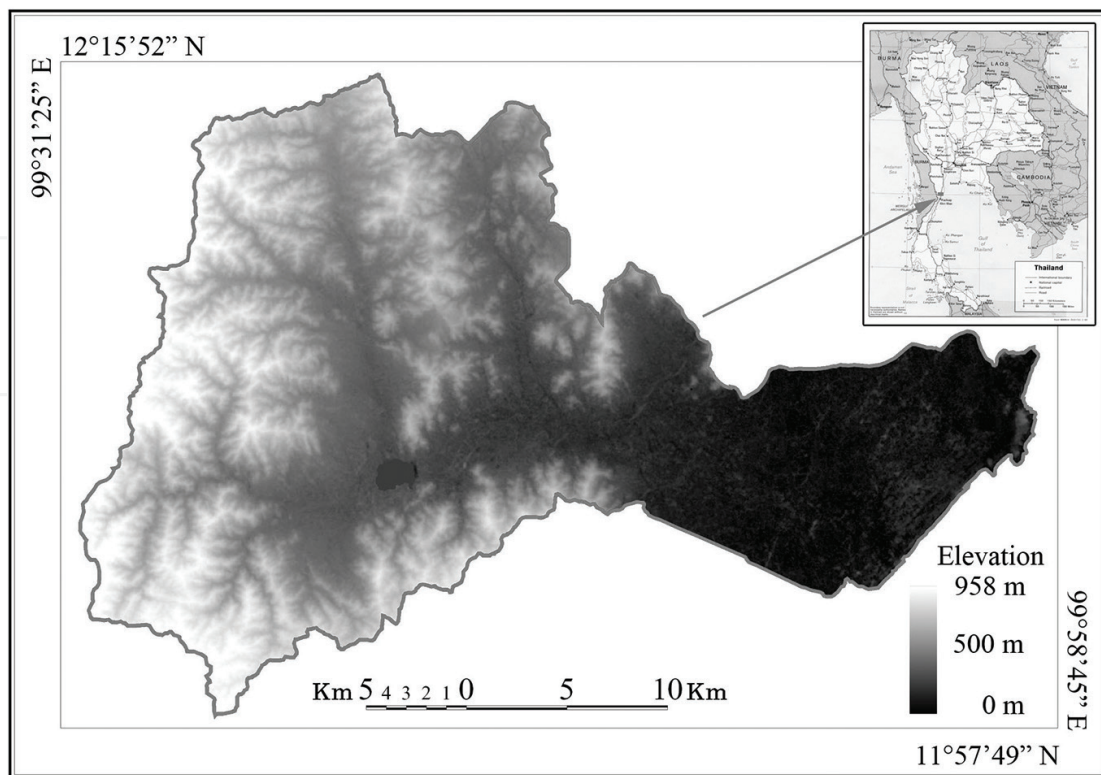


Figure 1. The study area in Khlong Kui watershed (ASTER GDEM is a product of METI and NASA).

Climate: The study area has a tropical savanna climate with drying season from January to May and raining season from June to December. The annual rainfall 30-year average is 1153 mm as the highest in November and the annual average temperature is 31.4°C as the highest in April [9]. Due to the highest rainfall in November, soil erosion and land slide might be occurred in the area where nonvegetation and bared land with high slope are the types of land use in Khlong Khui watershed.

2.2. Data use

In this study, Landsat 7 Enhanced Thematic Mapper (ETM) images in 1991, 2005 and Landsat 8 Operational Land Imager (OLI) and Thermal Infrared Sensor (TIRS) image in 2014 were used for land use and land cover (LULC) classification of the Khlong Kui watershed. A digital form of the watershed boundary was utilized. Field survey, topographic maps and LULC thematic maps were used for classification accuracy assessment. Digital Elevation Model (DEM), soil series digital maps and rainfall data were used as ancillary data to identify potential risk areas of soil erosion.

Landsat 7 ETM acquired on 02 Dec. 1991 and 17 Feb. 2005 were provided Global Land Cover Facility at Maryland University was available at <http://glcf.umd.edu/data/landsat/>

Landsat 8 OLI-TIRS image dated 02 Feb. 2014 was available at: <http://earthexplorer.usgs.gov>. The study area was covered by Landsat images with path 129/row 52. The multispectral bands contain spatial resolution at 30 × 30 m and the panchromatic band has spatial resolution at 15 × 15 m.

The Khlong Kui watershed boundary was GIS vector in ESRI Shape file that was derived from the Forest and Watershed Management Project in 2005 of the Royal Forest Department.

Topographic maps were acquired in 1995 from the Land Development Department, Thailand with a scale of 1:50,000.

LULC thematic maps were shape files for Prachuap Khiri Khan province that were created by the Land Development Department, Thailand with a scale of 1:50,000 (surveyed between 2000 and 2002).

Digital Elevation Model was Advanced Spaceborne Thermal Emission and Reflection Radiometer (ASTER) Global Digital Elevation Model (GDEM) 30 x 30 m that was provided by Japan Space Systems, Earth Remote Sensing Division, available at <http://gdem.ersdac.jspacesystems.or.jp/>.

Rainfall data were composed from The Tropical Rainfall Measuring Mission (TRMM) is a joint mission between National Aeronautics and Space Administration (NASA) and the Japan Aerospace Exploration Agency (JAXA) designed to monitor and study tropical rainfall. The rainfall measuring instruments on the TRMM satellite include the Precipitation Radar (PR), an electronic scanning radar operating at 13.8 GHz; TRMM Microwave Image (TMI), a nine-channel passive microwave radiometer; and Visible and Infrared Scanner (VIRS), a five-channel visible/infrared radiometer. The purpose updated algorithm is to produce the best-estimate precipitation rate (in mm/h) and root-mean-square (RMS) precipitation-error estimates from TRMM and other data sources [10]. Vertical hydrometeor profiles and surface rainfall means are computed monthly with the grid size as 0.5°×0.5°. The amounts of annual rainfall in the study area and its six categories with higher amount of rainfall were ranked with the higher scores (**Table 1**).

Factor	Ranking scores					
	1	2	3	4	5	6
Slope (%)	≤2.0	2–5	5–10	10–15	15–30	>30
Land use/land cover	Water bodies, urban and built-up land, and wetland	Deciduous forest	Evergreen forest	Rice field	Orchard	Cropland
Parent material	Very high resistant to water erosion (water bodies, rock land, igneous rock formations, more diorite, andesite, and basalt)	High resistant to water erosion (alluvial deposits of plains)	Moderate resistant to water erosion (various rock and metamorphic formations, quartzite, slate, phyllite, some andesite, and some shale)	Slight low resistant to water erosion (combination of metamorphic and sedimentary rock formations, quartzite, slate, phyllite, more sandstone and shale)	Low resistant to water erosion (sedimentary rock formations, more shale and limestone)	Very low resistant to water erosion (badland, residuum and colluviums form sandstone and old alluvium, rock mountainous and eroded land)
Rainfall (mm)	≤1000	1000–1150	1150–1300	1300–1450	1450–1600	>1600

Table 1. Factors ranking used in the model of risk assessment of soil erosion.

Soil series maps of six provinces that were collected during field work between 1999 and 2002 were created by Land Development Department, Thailand in the shape file format. They came with soil series' soil materials properties in the Excel format. The attributes of soil series' soil materials properties were in the Excel format which was standardized with type of lithology prepared by FAO (in 2006). The soil materials were graded into six classes based on their resistant to water as provided in **Table 1**.

Slope is shown as the percentage of slope gradient that was calculated from Triangulated Irregular Networks (TIN) come from Digital Elevation Model (DEM) by using the Spatial Analyst Surface. The slope gradient structures were classified into six classes in accordance with the slope gradient classes [11] and the slope classes for water erosion [12]. The classes were classified from 1 to 6 as presented in **Table 1**.

Land use/land cover in 2014 classified from Landsat 8 OLI-TIRS images that were reclassified into six LULC types based on the crop management factor values provided by Land Development Department, Thailand (in 2000). The ranking scores of LULC are described in **Table 1**.

2.3. Methods

This study was accomplished using three major procedures: image classification and analysis, modeling LULC changes in 23 years (during 1991–2014) and identification of potential risk areas of soil erosion in the Khlong Kui watershed described as shown in **Figure 2**.

2.3.1. Satellite image geometric correction

The geometric correction process geometrically converts the image coordinates from (x, y) into Universal Transverse Mercator (UTM) Zone 47P map projection coordinate by using eight ground control points (GCPs). For the purpose of and use change and soil erosion analysis, all the satellite image and maps must be registered in the same pixel size and map projection with precise overlaying together. The second-order polynomial transformation and cubic convolution are used for image registration. In this study, the GCPs have been collected during 10–20 April, 2014 by using GPS-GLONASS L1 receiver brand ASTECH model Promark 100.

2.3.2. Satellite image enhancement

With respect original multispectral data set, the color distortion of pan-sharpening technique is significant limitation as shown in **Figure 3**. The statistics analysis was used to evaluate the digital value and characteristic of original data before pan-sharpening transform with enhanced data after pan-sharpening transform.

2.3.3. Image classification and analysis

The Landsat satellite images described in the previous section were used to investigate LULC in the Khlong Kui watershed, Thailand in 1991, 2005 and 2014. The images were analyzed with the image processing software GEOMATICA Ver. 2013, a widely used image processing software package, which is often used to perform LULC classification of remotely sensed data.

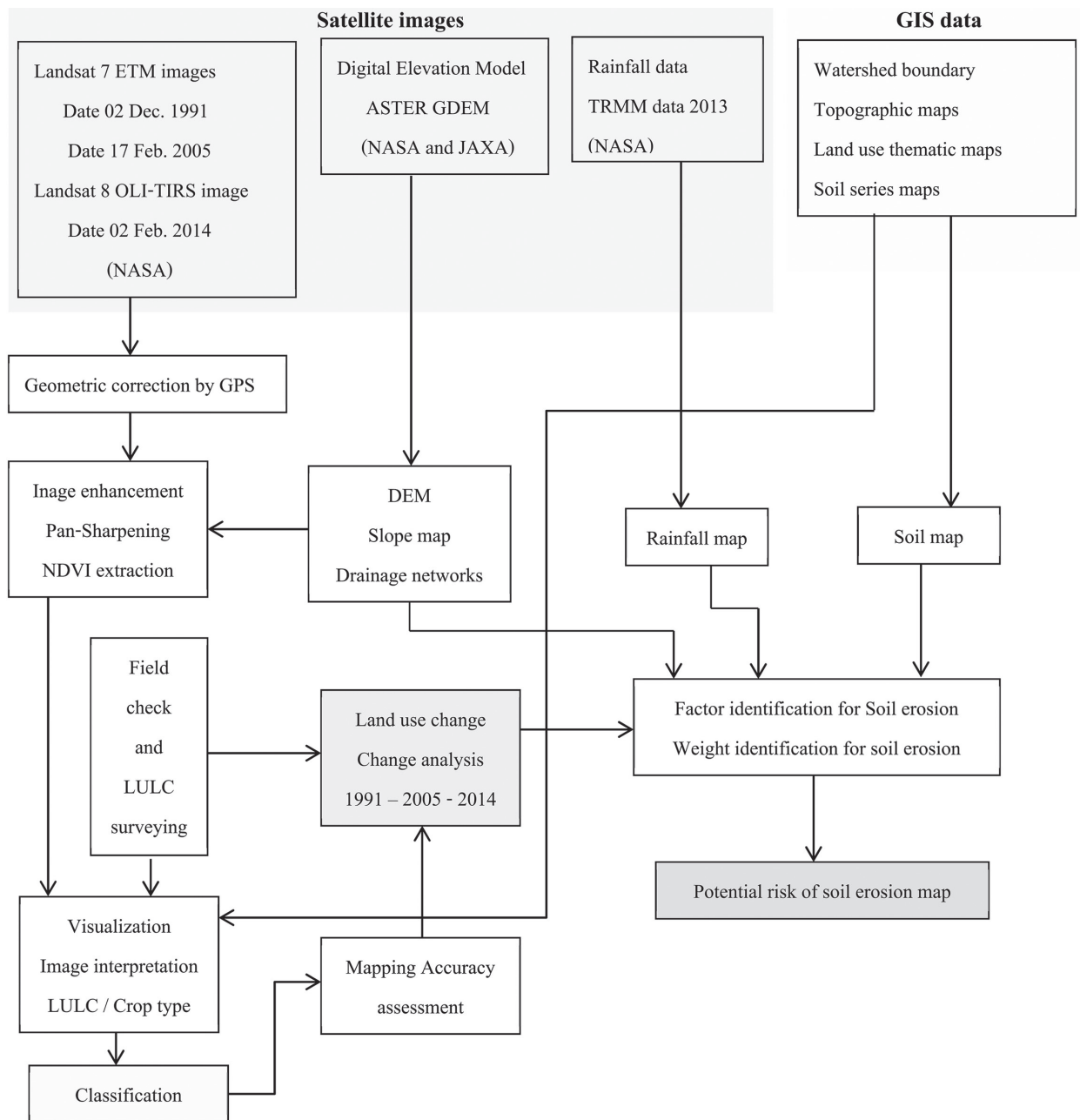


Figure 2. Methods for land use land cover classification and soil erosion risk mapping.

2.3.4. Image classification for land use and land cover map

Digital image classification is the process of recognizing pixels, which are given in multispectral bands of a satellite image. The process generates clusters of pixels with similar digital values into the same informational categories [8]. The classification performed by automated (unsupervised) or semiautomated (supervised) approaches are widely used in many LULC studies [1, 6, 13–16].

In this study, supervised method was used to classify LULC in the Khlong Kui watershed. Supervised classification employs samples of pixels that are already known informational categories to classify unknown pixels on an image. The class names were assigned into 12

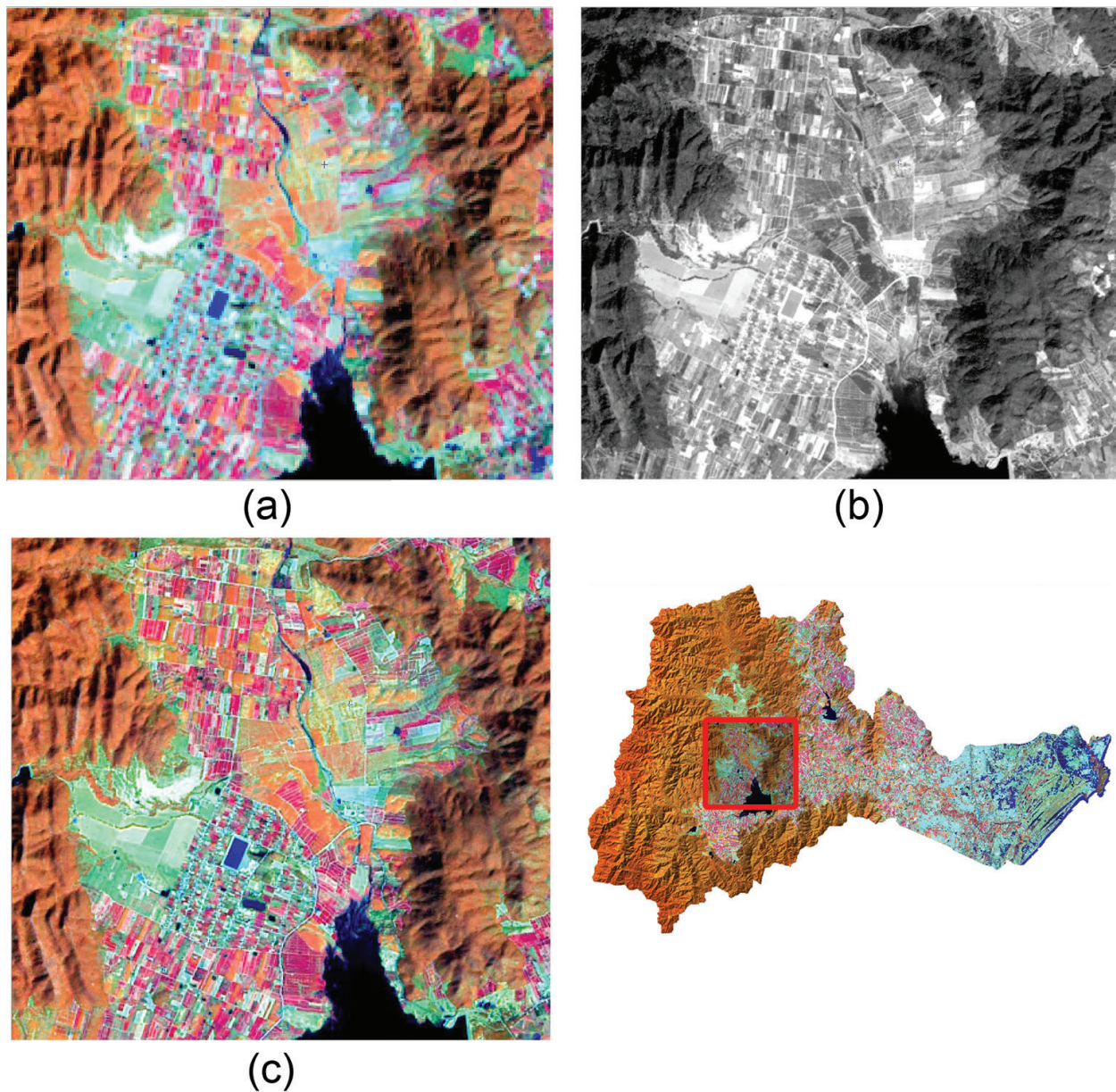


Figure 3. (a) Multi-spectral, (b) panchromatic channel and (c) pan-sharpening combination band 4-5-3 in R-G-B (Landsat imagery courtesy of NASA Goddard Space Flight Center and U.S. Geological Survey).

actual informational categories that are based on the 1976 USGS Land-Use and Land-Cover Classification [17] as (1) Urban villages (U11); (2) Cropland (A21); (3) Orchards (A22); (4) Rice field (A23); (5) Rangeland (R31); (6) Deciduous forest (F41); (7) Evergreen forest (F42); (8) Coastal forest (F43); (9) Water and reservoirs (W51); (10) Wetland (W61); (11) Barren land (B71) and (12) Beach (B72).

2.3.5. Ground truth and field checking for land use classification

Ground Truth and Field Checking for LULC classification was conducted during 10–20 April 2014 by identifying 100 locations as samples including main LULC as forest types, agricultural crops, rangeland and village area. The NEXUS 7 (Acer Tablet) with Android 4.4 combined

online Google map for navigating to the sample location by using 3G internet connection and GPS-GLONASS L1 receiver brand ASTECH model Promark 100. These samples were then applied for image classification accuracy assessment by generating classification confusion matrices and accuracy report.

2.3.6. Accuracy assessment

Accuracy assessment is an essential requirement of image classification, and it can be resulted by the confusion matrix. Confusion matrices quantitatively compare the relationship between the classified images and the reference data which contains field survey, high resolution digital map and/or thematic maps. After the confusion matrix is generated, overall accuracy, producer's and user's accuracies, omission and commission errors, and Kappa statistics [1, 15–18] can be written as shown in Eq. 1.

$$K = \frac{N \sum_{i=1}^r x_{ii} - \sum_{i=1}^r (x_{i+} \times x_{+i})}{N^2 - \sum_{i=1}^r (x_{i+} \times x_{+i})} \quad (1)$$

where N is the total number of sites in the matrix, r is the number of rows in the matrix, x_{ii} is the number in row i and column i , and x_{i+} is the total for column i , x_{+i} is the total for row i , [1].

LULC change analysis was conducted in three temporal periods: 1991–2005 and 2005–2014. Cross-tabulation table and cross-classification image were used for the change analysis. The cross-tabulation table presents the unchanging and changing frequencies of each LULC type by comparing pixels from the earlier classified image to the later one.

2.3.7. Identification of the potential risk areas of soil erosion

According to the literature, soil erosion of a land surface is caused by various factors. These factors include topography (e.g., slope orientation, steep and length), soil cover (e.g., trees, grasses, water, bare soil and paved surface), soil character (e.g., soil mass, soil components and soil materials), and climate (e.g., rainfall amount and intensity, temperature and wind) [7, 12, 19]. In this study, we chose four different factors based on data availability to identify the potential risk areas of soil erosion in the Khlong Kui watershed. These factors are (1) slope, (2) LULC, (3) soil parent material and (4) rainfall. To construct the model, we executed two processes: (1) variable ranking and layer creation and (2) model development.

2.3.8. Variable ranking and layer creation

The factors were categorized into six thresholds based on a review of the literature. The threshold categories were ranked from 1 as lower risk of soil erosion to 6 as higher risk of soil erosion as shown in **Table 1**.

2.3.9. Model development

The model was constructed using Multi-Criteria Modeling (MCM). MCM is an influential efficient technique for managing different types of ecological modeling for decision-making and

	Slope	LULC	Parent material	Rainfall	Weight calculation
Slope	1	7/5	7/3	7	0.3496
LULC	5/7	1	5/3	5	0.2496
Soil material	3/7	3/5	1	3	0.1496
Rainfall	1/7	1/5	1/3	1	0.0496

Table 2. A pairwise comparison matrix of the relative importance of erosion factors.

environmental planning [20, 21]. Weights for the erosion factors were derived from pairwise comparison by ranking the importance of each factor and comparing them with another as shown in **Table 2**.

Slope was ranked (as 7) as the most important factor because steep slope areas usually have high potential for soil erosion. However, different types of vegetation cover can prevent erosion; hence, LULC was ranked (as 5) as the second most important factor. Soil material and rainfall were ranked (as 3 and 1) as the third and the fourth important factors. The Fuzzy Logic method (IDRISI Software Ver.17) calculates the weights which were obtained by the relative importance matrix as 0.3496 for slope; 0.2496 for LULC; 0.1496 for soil material and 0.0496 for rainfall as displayed in **Table 2**.

The weights were then used to create two equations using the attribute calculator tool from software QGIS Ver. 2.6 as given in Eq. 2:

$$\text{Risk scores of soil erosion} = [\text{Slope}] \times 0.3496 + [\text{LULC}] \times 0.2496 + [\text{Soil_Material}] \times 0.1496 + [\text{Rainfall}] \times 0.0496 \quad (2)$$

The final risk scores of each model were standardized in percentage of potential risk by Eq. 3:

$$\% \text{potential risk of soil erosion} = \frac{X - \text{Min}}{\text{Max} - \text{Min}} \times 100 \quad (3)$$

where X is the final risk score, Min is the least score and Max is the highest score [12]. Finally, the percentages of potential risk of erosion were divided into five classes: very low (<20), low (20–40), moderate (40–60), high (60–80) and very high (>80) potential risk of soil erosion.

3. Results and discussions

3.1. LULC classification

The water and reservoir, deciduous forest, evergreen forest, rice field, urban and village land categories presented good classification performance during the study period. Based on the ground truth and field check data of 100 samples for LULC types, the classification assessment with the confusion matrices were generated for evaluating the overall, producer and user accuracy of each LULC types. As we can see in the confusion matrix as shown in **Table 3**,

Classified data	Reference data												Classified overall	Producer accuracy (%)
	U11	A21	A22	A23	R31	F 41	F 42	F 43	W 51	W61	B 71	B 72		
U11	3	0	0	0	0	0	0	0	0	0	0	0	3	100.00
A21	0	11	0	1	0	0	0	0	0	0	0	0	12	91.67
A22	0	3	10	1	0	0	0	0	0	0	0	0	14	71.43
A23	0	1	2	8	0	0	0	0	0	0	0	0	11	72.73
R31	1	0	0	0	5	0	0	0	0	0	2	0	8	62.50
F41	0	0	0	0	0	28	1	0	0	0	0	0	29	96.55
F42	0	0	0	0	0	0	19	1	0	0	0	0	20	95.00
F43	0	0	0	0	0	0	0	0	0	0	0	0	0	No data
W51	0	0	0	0	0	0	0	0	2	0	0	0	2	100.00
W61	0	0	0	0	0	0	0	0	0	0	0	0	0	No data
B71	1	0	0	0	0	0	0	0	0	0	0	0	1	0.00
B72	0	0	0	0	0	0	0	0	0	0	0	0	0	No data
True overall	5	15	12	10	5	28	20	1	2	0	2	0	100	
User accuracy (%)	60.00	73.33	83.33	80.00	100.00	100.00	95.00	0.00	100.00	No data	0.00	No data		
Overall accuracy:	86%													
Overall Kappa statistic:	0.831													

Table 3. LULC classification 2014 Feb 02: confusion matrix.

water and reservoir archived 100% for both producer and user accuracy because the signature of water is sufficient difference from vegetation and other land cover types. Deciduous forest and evergreen forest are also classified with high accuracy as 96 and 95% for producer accuracy and 100 and 95% for user accuracy, respectively. The cropland (91.67% producer accuracy, 73.33% user accuracy) and orchard (71.43% producer accuracy and 83.333 user accuracy) categories had moderate classification performance. Rangeland (62% producer accuracy) had lower accuracy as it was mixed with barren land and urban village type. The wetland category had poor classification performance except in the 2005 classified image where it had high accuracy performance. The uncertainty of classification among forests, agricultural lands and wetlands occurred due to similar spectral reflectance of green vegetation. This confusion usually occurs when using moderate spatial resolution images such as Landsat satellite images to classify areas that have heterogeneous LULC [22].

For the overall classification accuracy of the 1991, 2005 and 2014 images, a satisfactory accuracy of more than 80% was achieved with 100 reference samples. LULC classification resulted in overall accuracy at 80% for 1991, 83% for 2005 and 86% for 2014 and Kappa Statistic at 8.83, 0.79 and 0.76 for 2014, 2005 and 1991, respectively as seen in the confusion matrix as shown

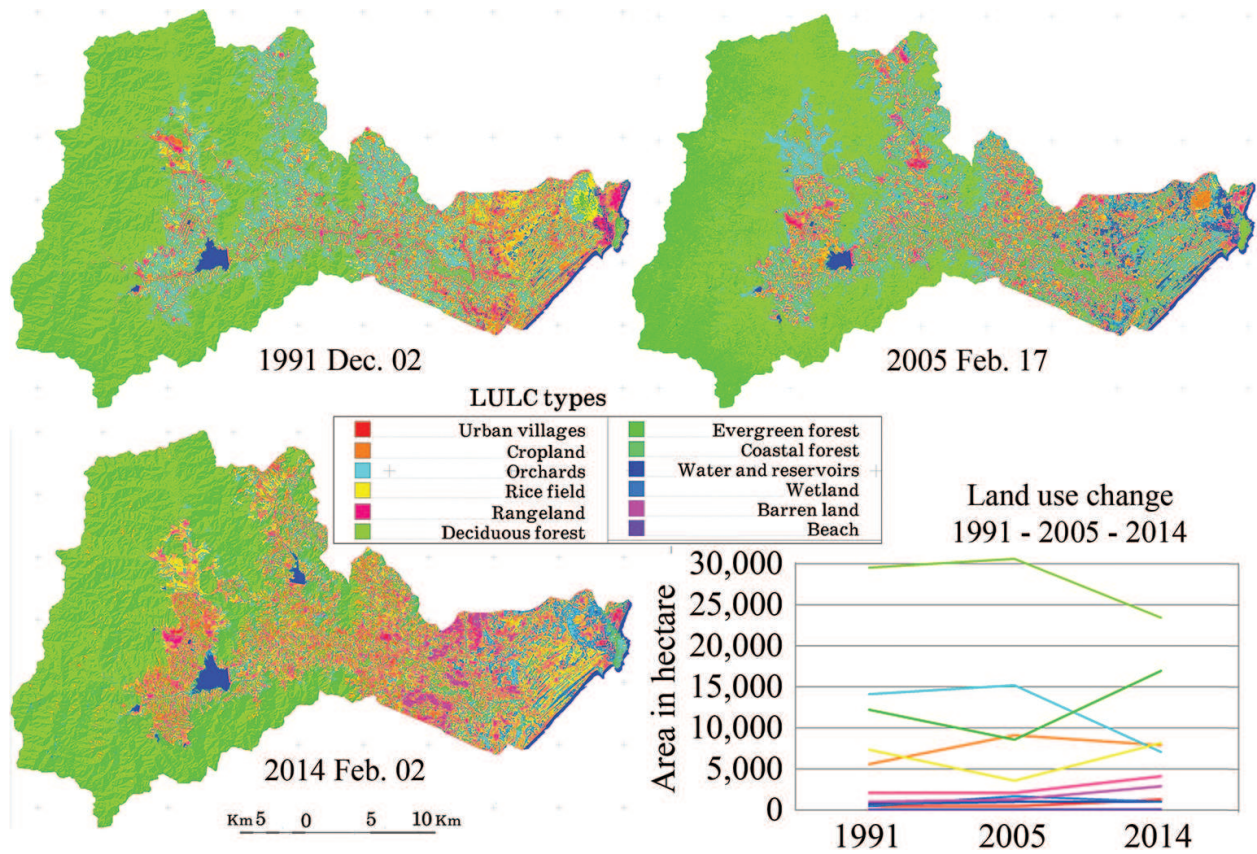


Figure 4. Land use land cover classification in 1991, 2005 and 2014.

Code	LULC types	Area in percentage			
		1991 Dec. 02	2005 Feb. 17	2014 Feb. 02	Change 1991-2014
U11	Urban villages	0.65	0.64	1.66	1.003
A21	Cropland	7.63	12.39	10.64	3.015
A22	Orchards	19.09	20.53	9.69	-9.404
A23	Rice field	9.93	4.92	11.05	1.120
R31	Rangeland	2.79	2.83	5.60	2.811
F41	Deciduous forest	40.12	41.42	31.84	-8.281
F42	Evergreen forest	16.64	11.66	22.96	6.327
F43	Coastal forest	0.04	0.02	0.02	-0.015
W51	Water and reservoirs	0.96	1.43	1.32	0.364
W61	Wetland	0.70	2.34	1.27	0.576
B71	Barren land	1.44	1.81	3.92	2.475
B72	Beach	0.01	0.01	0.02	0.009
	Total	100.00	100.00	100.00	

Table 4. Summary of land use land cover changes from 1991 Dec. to 2014 Feb. in Klong Kui watershed.

	Code	U11	A21	A22	A23	R31	F41	F42	F43	W51	W61	B71	B72	Total
LULC in 1991 area (ha)														
LULC in 2005	U11	46.42	62.93	117.41	66.08	45.88	26.42	1.55	0.54	11.07	6.53	36.05	0.61	421.47
	A21	90.43	1753.38	3480.39	1789.65	502.52	1036.73	91.31	0.97	76.10	62.26	233.24	0.41	9117.36
	A22	84.06	2041.34	6151.68	2644.72	439.83	3761.01	132.05	0.38	50.87	123.95	205.70	0.05	15,635.64
	A23	65.84	601.58	1058.18	607.91	316.80	224.69	21.29	4.57	46.94	31.50	183.26	0.38	3162.92
	R31	37.13	344.12	694.40	293.92	155.12	172.13	5.20	0.07	6.68	6.53	90.63	0.02	1805.92
	F41	12.74	369.77	1865.99	621.56	61.70	20,262.30	7930.80	0.92	17.03	37.06	32.04		31,211.90
	F42	1.13	12.13	150.71	28.08	4.93	4217.90	3780.32	0.09	2.72	5.92	2.68		8206.59
	F43				0.11	2.63		0.14	6.50	1.22	0.00	0.20	0.23	11.03
	W51	29.45	68.24	56.61	208.35	76.93	12.83	18.79	5.72	606.93	116.42	33.62	2.12	1235.99
	W61	32.51	243.47	271.46	604.71	149.06	78.77	63.68	2.09	66.98	86.65	61.04		1660.43
	B71	76.01	183.26	415.80	176.69	144.25	87.91	2.57	1.82	16.47	9.90	106.90	0.70	1222.27
	B72	0.86				0.32		0.07	2.30	0.29	0.00	0.09	4.57	8.48
	Total	476.55	5680.22	14,262.62	7041.78	1899.95	29,880.67	12,047.74	25.97	903.30	486.70	985.43	9.07	73,700.00
	LULC in 2005 area (ha)													
LULC in 2014	U11	46.60	214.18	205.58	129.33	102.89	37.78	2.48	0.25	14.81	23.99	73.31	0.18	851.36
	A21	52.83	1943.06	3319.56	609.71	321.55	812.57	43.43	0.79	33.77	178.63	213.32	0.56	7529.77
	A22	48.04	1049.63	2934.59	406.98	150.26	1549.49	129.02	2.18	276.23	545.47	127.55	0.56	7220.00
	A23	82.42	2805.39	3847.86	718.74	472.82	616.55	27.50	0.32	43.38	192.35	275.02		9082.33
	R31	65.77	1240.56	1128.38	437.56	341.01	198.11	12.76		22.77	95.24	164.95		3707.11
	F41	16.07	852.37	2934.05	246.04	149.54	15,104.70	4503.02		0.11	14.02	96.41		23,916.32
	F42	3.92	90.36	380.43	29.16	12.42	12,625.00	3473.91	0.32	11.41	126.92	14.69	0.05	16,768.58
	F43	0.34			4.19	0.02	0.05	0.00	5.04	3.22	0.41	2.72	0.61	16.58
	W51	29.50	138.17	77.24	92.36	32.99	23.87	6.37	0.29	668.69	53.46	46.62	3.15	1172.71
	W61	14.51	101.14	130.91	141.32	15.32	54.74	1.40	0.00	110.23	286.99	43.63		900.18
	B71	62.08	678.47	674.69	346.39	207.92	174.51	5.83	0.27	67.97	139.23	160.74		2518.09
	B72	0.65	3.08	0.18	3.13	0.14			1.49	0.63	1.06	3.33	3.31	16.99
	Total	422.71	9116.40	15,633.47	3164.90	1806.86	31,197.36	8205.69	10.94	1253.22	1657.76	1222.29	8.42	73,700.00

Table 5. Land use land cover change analysis from 1991 to 2014.

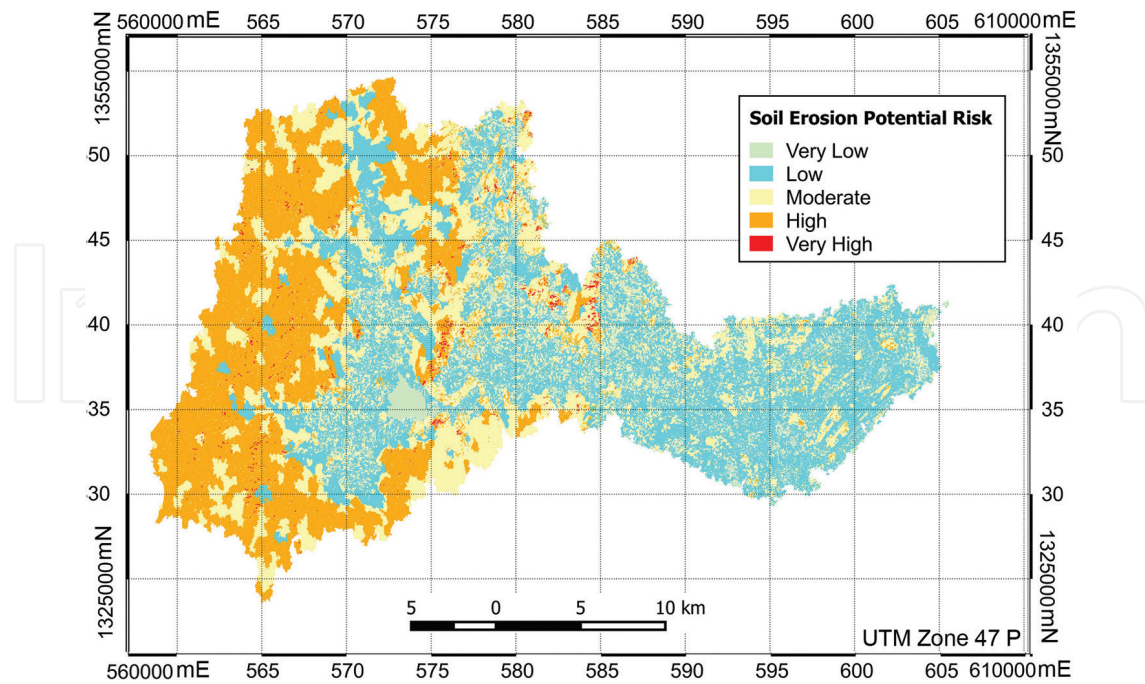


Figure 5. Khlong Kui watershed: Potential soil erosion risk map.

in **Table 3**. These overall accuracies are decreased for old dated data (1991 and 2005) due to many changes in forest and agricultural land use in comparison with those identified during ground truth period. The LULC types are presented in **Figure 4**, and the statistics of area is calculated in **Table 4**.

3.2. LULC changes and analysis (1991–2014)

The gains and losses are shown in **Figure 4**, and the cross tabulation of the changes between 1991 and 2014 (**Table 5**) is reliable with the previous two periods (1991–2005 and 2005–2014). Although there were gains in evergreen forests (6.32%) from croplands, orchards, barren land and deciduous forests, the great loss of deciduous forests (–8.28%) occurred due to conversion to evergreen forests, rangeland, barren land and croplands. Moreover, **Table 5** shows that the increase of evergreen forests, rice fields and croplands (3.01%) was mainly from deciduous forests. Most of the orchard losses (–9.40%) were converted to evergreen forests, barren land and croplands.

The major loss of coastal forest (–0.01%) was due to conversion to deciduous forests. Although the minor changes among LULC types could have followed by a result of agricultural activities such as shifting cultivation, crop rotation and infrastructure development and some of these changes could be added to the error of classification caused by similar spectral reflectance or mixed pixels from the various characteristic of LULC in the region.

3.3. Identification of the potential risk areas of soil erosion

Fuzzy Logic presented a major weighting factor in development of the model because mountains are a major landscape of the watershed. The results from Fuzzy Logic seem to be more

conventional based on the topography of the watershed with very high risk (0.63%), high risk (32.00%), moderate risk (32.40%), low risk (31.21%) and very low risk (3.76%) as shown in **Figure 5**. The clusters of very high risk were consistent with the northern, central, eastern regions of the watershed as also presented in **Figure 5**. They were mainly located in mountainsides or hillsides, which are usually steep slope and boundaries between forests and highland crops.

In general, most areas of the Khlong Kui watershed had high potential risk of soil erosion due to the combination of mountainous topography and agricultural activities. High rainfall in high mountain area generated more areas of higher risk while low rainfall in low and flat area generated areas of lower risk.

4. Conclusions

This study used remote sensing and GIS techniques to assess land use and land cover (LULC) and its dynamics of change with identify the potential risk areas of soil erosion in the Khlong Kui watershed in 1991, 2005 and 2014. The Khlong Kui watershed was selected as the study area because this watershed has been experiencing deforestation and soil degradation due to the development of agricultural lands and urban areas. Moreover, the topography of the watershed, which includes mountains, hills and slopping lands, makes the Khlong Kui watershed an interesting region to examine potential risk areas of soil erosion. The key findings of the research are as follows:

4.1. Image classification and analysis

The major LULC of the Khlong Kui watershed are forests and agricultural lands. The study monitored an increase in orchards, croplands, evergreen forests, rice field and urban areas while a decrease in deciduous forests and wetlands in the watershed in 1991, 2005 and 2014. The overall accuracy assessment of the image classification was satisfactory in all three different years of satellite data acquisition.

4.2. LULC changes and dynamics

Deciduous forest, evergreen forest and orchards types were major drivers of land use and land cover changes. An increase of range land, croplands and evergreen forests were mainly derived from deciduous forests. The development of range land, barren land and crop land was related to an increase in infrastructure of the Khlong Kui watershed. There is a high probability of change from deciduous forests, wetlands and orchards to rice fields and croplands in 2014.

4.3. Potential risk areas of soil erosion

High-risk areas of soil erosion were primarily located in the northern and eastern regions of the watershed which are also with mountain ranges and hilly areas. High rainfall in high mountain area generated more areas of very high risk at 0.63% of the watershed. The change

from forests to agricultural lands in the northwestern and northeastern regions of the watershed led to higher risk areas of soil erosion in the last 9 years.

4.4. Recommendation for further research

Due to limitation of research, financial budget and time, land use change and soil erosion model have lacked sample questionnaire for validation process. It is recommended for further research works that develop an additional surveying method to improve the soil erosion model to archive more accurate and creditable result.

Acknowledgements

The ASTER L1B data product was obtained through the online Data Pool at the National Aeronautics and Space Administration (NASA) Land Processes Distributed Active Archive Center (LP DAAC), USGS/Earth Resources Observation and Science (EROS) Center, Sioux Falls, South Dakota (https://lpdaac.usgs.gov/data_access).

The data used in this study were acquired as part of the Tropical Rainfall Measuring Mission (TRMM). The algorithms were developed by the TRMM Science Team. The data were processed by the TRMM Science Data and Information System (TSDIS) and the TRMM office; they are archived and distributed by the Goddard Distributed Active Archive Center. TRMM is an international project jointly sponsored by the Japan National Space Development Agency (NASDA) and the US-NASA Office of Earth Sciences.

This research was supported by the Department of Civil Engineering, Faculty of Engineering, Rajamangala University of Technology Rattanakosin, WangKlaiKangWon Campus, Prachuab Khirikhan, Donor. We would like to thank Rajamangala University of Technology Rattanakosin, WangKlaiKangWon Campus for its financial support and providing facilities to make this research possible. We would also like to thank the National Aeronautics and Space Administration (NASA), Land Processes Distributed Active Archive Center (LP DAAC), USGS/Earth Resources Observation and Science (EROS) Center, Sioux Falls, South Dakota (https://lpdaac.usgs.gov/data_access) for providing the ASTER L1B data product. We would also express our gratitude to the Goddard Distributed Active Archive Center that delivers TRMM for this research. TRMM is an international project jointly sponsored by the Japan National Space Development Agency (NASDA) and the US-NASA Office of Earth Sciences.

Author details

Patchareeya Chaikaew

Address all correspondence to: patchareeya.cha@rmutr.ac.th

Department of Civil Engineering, Faculty of Engineering, Rajamangala University of Technology Rattanakosin, Prachuap Khiri Khan, Thailand

References

- [1] Jensen JR. *Introductory Digital Image Processing: A Remote Sensing Perspective*. New Jersey: Pearson Education, Inc; 2005. pp. 107-312
- [2] Turner BL, Lambin EF, Reenberg A. The emergence of land change science for global environmental change and sustainability. *Proceedings of the National Academy of Sciences (PNAS)*. 2007;**104**(52):20666-20671
- [3] Delang CO. Deforestation in northern Thailand: The result of Hmong farming practices of Thai development strategies? *Society and Natural Resources*. 2002;**15**:483-501
- [4] OAE. Office of Agricultural Economics: Land Use Statistics. 2014. Available from: http://www.oae.go.th/download/use_soilNew/soiNew/landused2554.html [Accessed: 2014-03-14]
- [5] Longley PA, Goodchild MF, Maguire DJ, Rhind DW. *Geographic Information Systems and Science*. England: John Wiley & Sons, Ltd.; 2005. pp. 364-382
- [6] Fromard F, Vega C, Proisy C. Half a century of dynamic coastal affecting mangrove shoreline of French Guiana: A case study based on remote sensing data analyses and field surveys. *Marine Geology*. 2004;**208**:265-280
- [7] Sidle RC, Ziegler AD, Negishi JN, Nik AR, Siew R, Turkelboom F. Erosion processes in steep terrain—Truths, myths, and uncertainties related to forest management in Southeast Asia. *Forest Ecology and Management*. 2006;**224**:199-225
- [8] BC J, Randolph HW. *Introduction to Remote Sensing*. New York: The Guilford Press; 2011. pp. 335-375
- [9] TMD 2014. Thai Meteorological Department. Available from: http://www.tmd.go.th/en/province_stat.php?StationNumber=48500 [Accessed: 2014-03-02]
- [10] Wu H, Adler RF, Tian Y, Huffman GJ, Li H, Wang J. Real-time global flood estimation using satellite-based precipitation and a coupled land surface and routing model. *Water Resources Research*. 2014;**50**:2693-2717
- [11] FAO. *Guidelines for Soil Description*. Rome: FAO; 2006. pp. 126-284
- [12] Masoudi M, Patwardhan AM, Gore SD. A new methodology for producing of risk maps of soil salinity, case study Payab Basin, Iran. *Journal of Applied Sciences and Environmental Management*. 2006;**10**(3):9-13
- [13] Muttitanon W, Tripathi NK. Land use/land cover changes in the coastal zone of Ban Don Bay, Thailand using Landsat 5 TM data. *International Journal of Remote Sensing*. 2005; **26**(11):2311-2323
- [14] Joao BC, Jose CP, Yosio ES. Land-cover mapping in the Brazilian Amazon using SPOT-4 vegetation data and machine learning classification methods. *Photogrammetric Engineering & Remote Sensing*. 2006;**72**(8):897-910

- [15] Lillesand T, Kiefer RW, Chipman JW. Remote Sensing and Image Interpretation. United States: John Wiley & Sons, Inc; 2007. pp. 302-476
- [16] Lu D, Weng Q. A survey of image classification methods and techniques for improving classification performance. *International Journal of Remote Sensing*. 2007;**28**(5):823-870
- [17] Anderson JR, Hardy EE, Roach JT, Witmer RE. A Land Use and Land Cover Classification for Use with Remote Sensor Data. USGS Professional Paper 964. Washington, DC: US Government Printing Office; 1976
- [18] Sirikulchayanon P, Sun W, Oyana TJ. Assessing the impacts of the 2004 tsunami on mangroves using GIS and remote sensing techniques. *International Journal of Remote Sensing*. 2008;**29**(12):3553-3576
- [19] Sang-Arun J, Mihara M, Horaguchi Y, Yamaji E. Soil erosion and participatory remediation strategy for bench terraces in northern Thailand. *Catena*. 2006;**65**:258-264
- [20] Clark JG, Jessica G. Tracking lyme disease: A hybrid approach to assess potential locations of risk in Jackson County, Illinois [Master thesis]. Carbondale: Southern Illinois University Carbondale; 2006. pp. 153-196
- [21] Baja S, Chapman DM, Dragovich D. Spatial based compromise programming for multiple criteria decision making in land use planning. *Environmental Modeling and Assessment*. 2007;**12**:171-184
- [22] Ibrahim O, Barabara K, Asan U, Gross CP, Hemphill S. Separation of citrus plantations from forest cover using Landsat imagery. *Allgemeine Forst Und Jagdzeitung*. 2007;**178** (11/12):208-212

